RESEARCH ARTICLE

The interplay between vaccination and social distancing strategies affects COVID19 population-level outcomes

Sharon Guerstein[1], **Victoria Romeo-Aznar**[2,3], **Ma'ayan Dekel**[1], **Oren Miron**[4], **Nadav Davidovitch**[4], **Rami Puzis**[5], **Shai Pilosof**[1]*

1 Department of Life Sciences, Ben-Gurion University of the Negev, Beer-Sheva, Israel, **2** Department of Ecology & Evolution, University of Chicago, Chicago, Illinois, United States of America, **3** Department of Ecology, Genetics & Evolution, and IEGEBA (UBA-CONICET), Faculty of Exact and Natural Sciences, University of Buenos Aires, Buenos-Aires, Argentina, **4** School of Public Health, Faculty of Health Sciences, Ben-Gurion University of the Negev, Beer-Sheva, Israel, **5** Software and Information Systems Engineering, Ben-Gurion University of the Negev, Beer-Sheva, Israel

* pilos@bgu.ac.il

Abstract

Social distancing is an effective population-level mitigation strategy to prevent COVID19 propagation but it does not reduce the number of susceptible individuals and bears severe social consequences—a dire situation that can be overcome with the recently developed vaccines. Although a combination of these interventions should provide greater benefits than their isolated deployment, a mechanistic understanding of the interplay between them is missing. To tackle this challenge we developed an age-structured deterministic model in which vaccines are deployed during the pandemic to individuals who do not show symptoms. The model allows for flexible and dynamic prioritization strategies with shifts between target groups. We find a strong interaction between social distancing and vaccination in their effect on the proportion of hospitalizations. In particular, prioritizing vaccines to elderly (60+) before adults (20-59) is more effective when social distancing is applied to adults or uniformly. In addition, the temporal reproductive number R_t is only affected by vaccines when deployed at sufficiently high rates and in tandem with social distancing. Finally, the same reduction in hospitalization can be achieved via different combination of strategies, giving decision makers flexibility in choosing public health policies. Our study provides insights into the factors that affect vaccination success and provides methodology to test different intervention strategies in a way that will align with ethical guidelines.

Author summary

A major question in epidemiology is how to combine intervention methods in an optimal way. With the recent deployment of COVID19 vaccine, this question is now particularly relevant. Using a data-driven model in which vaccines are deployed during the pandemic and their prioritization can shift between target groups we show that there is a strong interplay between these interventions. For example, prioritizing vaccines to elderly—the

common strategy worldwide—results in a larger reduction in hospitalizations when social distancing is applied to adults than to elderly. Importantly, reduction in hospitalizations can be achieved via multiple combination of intervention strategies, allowing for flexible public health policies.

Introduction

Vaccines are an essential tool for reducing the burden of endemic diseases such as measles, hepatitis, and influenza. For such diseases, vaccine development and production is, by now, a well-practiced process. Nevertheless, developing, producing, and deploying vaccines in the midst of a pandemic is a great challenge. For example, during the H1N1 pandemic vaccines were limited and their deployment required prioritization [1]. COVID19 is a typical example of such a situation. Without vaccines, the only strategy to contain COVID19 is to cut transmission chains by reducing contacts. Public health measures such as social distancing, improved hygiene, and face masks effectively reduce the risk of infection but do not reduce susceptibility among the population. Moreover, social-distancing interventions also bear social, economic, and psychological consequences [2, 3]. Therefore, vaccine development for COVID19 has been carried out at an unprecedented pace. Nevertheless, even now, when a vaccine is available, its deployment requires prioritization due to high demand and low supply. Thinking ahead about relevant strategies for deployment may save not only valuable time for policy makers [1, 4], but eventually lives and it is therefore at the forefront of debate and research [5–9].

Social distancing is the main strategy we currently have to deal with silent infections. Therefore, it is crucial to consider the interplay between vaccination and social distancing because, even when a vaccine is deployed, social-distancing is still enforced at some level. Several studies have examined vaccination strategies [6, 10–14], addressing multiple aspects of this issue. While these studies vary in their modeling frameworks, a general emerging result is that vaccines should be prioritized to the elderly and essential workers. Yet no study that we know of has explicitly tested the interplay between these two interventions in a realistic scenario in which vaccines are deployed according to a prioritization strategy. A mechanistic understanding of this interplay can serve to hone adequate strategies and understand possible caveats with a particular choice of strategy.

Here, we examine combinations of vaccine deployment and social distancing, and the interaction between them, using a data-driven, age-structured, deterministic model. We implement vaccination dynamics that reflect real-world scenarios by deploying vaccines to individuals who, in the eye of public health, are susceptible: presymptomatic and asymptomatic (exposed and infectious), those that have recovered from an asymptomatic infection, and susceptible individuals (those who were never infected). We model a scenario in which vaccines are deployed while social distancing is still in place—a highly likely situation in every country. Our goal is to illuminate qualitative effects of the interplay between vaccine deployment and social distancing. Which strategy combination can minimize adverse outcomes, and how? We focus on reduction in hospitalizations because hospital care is a limited resource in public health, which is also correlated with mortality. We show that the interplay between these interventions can have a synergistic effect. Moreover, the same reduction in hospitalization can be achieved via different combination of strategies, giving decision makers flexibility in choosing public health policies. These results were consistent for four countries.

Results

We developed an age-structured deterministic compartmental model that reflects the main states of COVID19 progression, including a presymptomatic stage, which has been shown to affect transmission and possible control efforts [15, 16] (Fig 1 and S1 Fig). We used 10-yr interval age-grouping (0–9, 10–19,. . .,70–79,80+), in line with previous studies of COVID19 (e.g, [17]) and with the data management protocols of most countries. The model and choice of parameter values are detailed in the Methods.

Vaccines are deployed at a constant rate of κ vaccines per day, which we measure as the percentage of population that a government can vaccinate a day (e.g., $\kappa = 0.2$ translates to deployment of 16,000 vaccines per day in a population of 8 million people). The amount of daily vaccines is divided proportionally to the size of the target age groups. Following [18] we apply an 80% vaccination acceptance proportion for the target groups. We explore two vaccination strategies: (i) 'elderly first', in which elderly (ages 60+) are vaccinated first and adults (20–59)
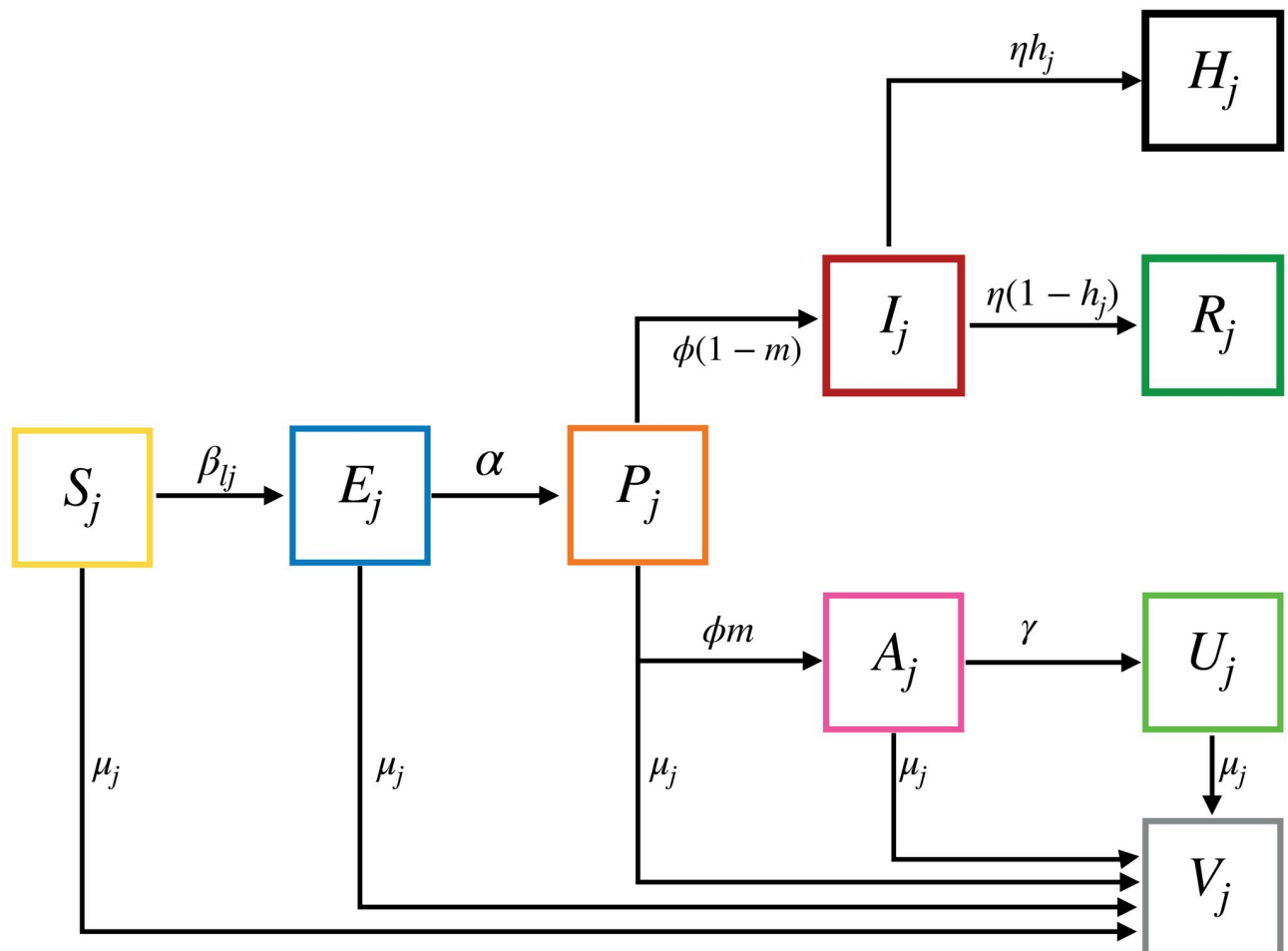

Fig 1. Model description. Individuals transition between states with rates specified by Greek letters. Small Latin letters are probabilities. Subscripts j and l depict age groups. Individuals start at a susceptible state (S) and upon infection with an age-dependent rate β_{lj} become infected with the virus (E). After an incubation period of $1/\alpha$ days individuals become presymptomatic (P) for $1/\phi$ days and infectious. The disease can then progress to be either asymptomatic (A) with a probability m, or symptomatic (I). Symptomatic individuals are identified and removed to quarantine (R) within $1/\eta$ days or, with a given age-dependent probability h_j develop severe symptoms and go to the hospital (H). Asymptomatic individuals naturally recover (U) within $1/\gamma$ days. All individuals that do not show symptoms can get a vaccine (V) at a constant rate of μ vaccines per day. See Methods for a comprehensive description of the model equations, parameters and vaccination strategies. See examples of model run in (S1 and S2 Figs).

next, and (ii) 'adults first', in which adults are vaccinated before elderly (S3 Fig). The elderly first strategy is currently being applied in most countries that have started vaccination campaigns (e.g., Israel). Once the prioritized age group is fully vaccinated, the vaccines are applied to the next group (S2 and S3 Figs). Vaccines are currently not developed for children and we therefore did not include ages 0–19 in vaccination strategies.

We present results in the main text for Israel, a small country of ≈ 8.7 million people, but we also tested our model using age demographics and contact matrices for Italy, Belgium and Germany, and results were qualitatively the same for all countries (see Sensitivity Analyses in Methods).

Social distancing affects vaccination strategies non-linearly

A combination of social distancing and vaccination is expected to have a synergistic, stronger effect in decreasing hospitalizations than any of these measures alone, and this effect should increase with stronger social distancing and higher vaccination rates. However, it is unclear how this interplay will be affected by vaccination rates and the strategy of social distancing. To test this, we apply social distancing either uniformly, to all the population regardless of age, or in a targeted way towards elderly or adults. We impose social distancing by reducing contact rates of specific ages (see Methods). We measure the impact of vaccine deployment as the percent of reduction in hospitalizations (in all the population) compared to a no-vaccination scenario as

$$F_H = 1 - \frac{\sum_j H_{j(\kappa)}}{\sum_j H_j^0}, \tag{1}$$

where $H_{j(\kappa)}$ is the total cumulative number of hospitalizations in age group j for a given deployment rate κ, and H_j^0 is the total number of hospitalizations in age group j when a vaccine is not deployed (S4 Fig).

As expected, vaccine impact increases with increasing vaccination rates (line colors in Fig 2). Prioritizing vaccines to adults does not reduce hospitalizations as effectively as when prioritizing to elderly (compare left to right columns in Fig 2). However, there is a strong interaction between vaccination and social distancing strategies in their effects on F_H. Combining an elderly first strategy with adult-targeted or uniform social distancing increases F_H in a non-linear, synergistic way (Fig 2A and 2C), while targeting both interventions at the elderly is not as effective (Fig 2B). In fact, when both interventions are targeted at the same group (elderly or adults), F_H varies very little or decreases with increasing strength of social distancing (Fig 2B and 2D). This is because strong social distancing by itself can prevent hospitalizations, overriding the need for vaccinations (as long as it is applied). This phenomenon also explains the decrease in F_H when social distancing is applied to all the population too strongly (Fig 2C and 2F).

Proportion hospitalized is determined by the interplay between intervention strategies

Because we find that social distancing can affect vaccination deployment efficiency, we now turn to quantify the joint effects of these interventions on the proportion of the population hospitalized across ages (depicted as P_H). To illustrate this, we first focus on a scenario in which $\kappa = 0.5$ as an example (Fig 3 and S5 Fig). We find that increasing levels of social distancing can have different effects on P_H, depending on the targeted groups. For example, targeting social distancing at elderly under an adults first vaccination strategy reduces P_H more effectively than under an elderly first strategy (compare trends in purple lines in Fig 3).
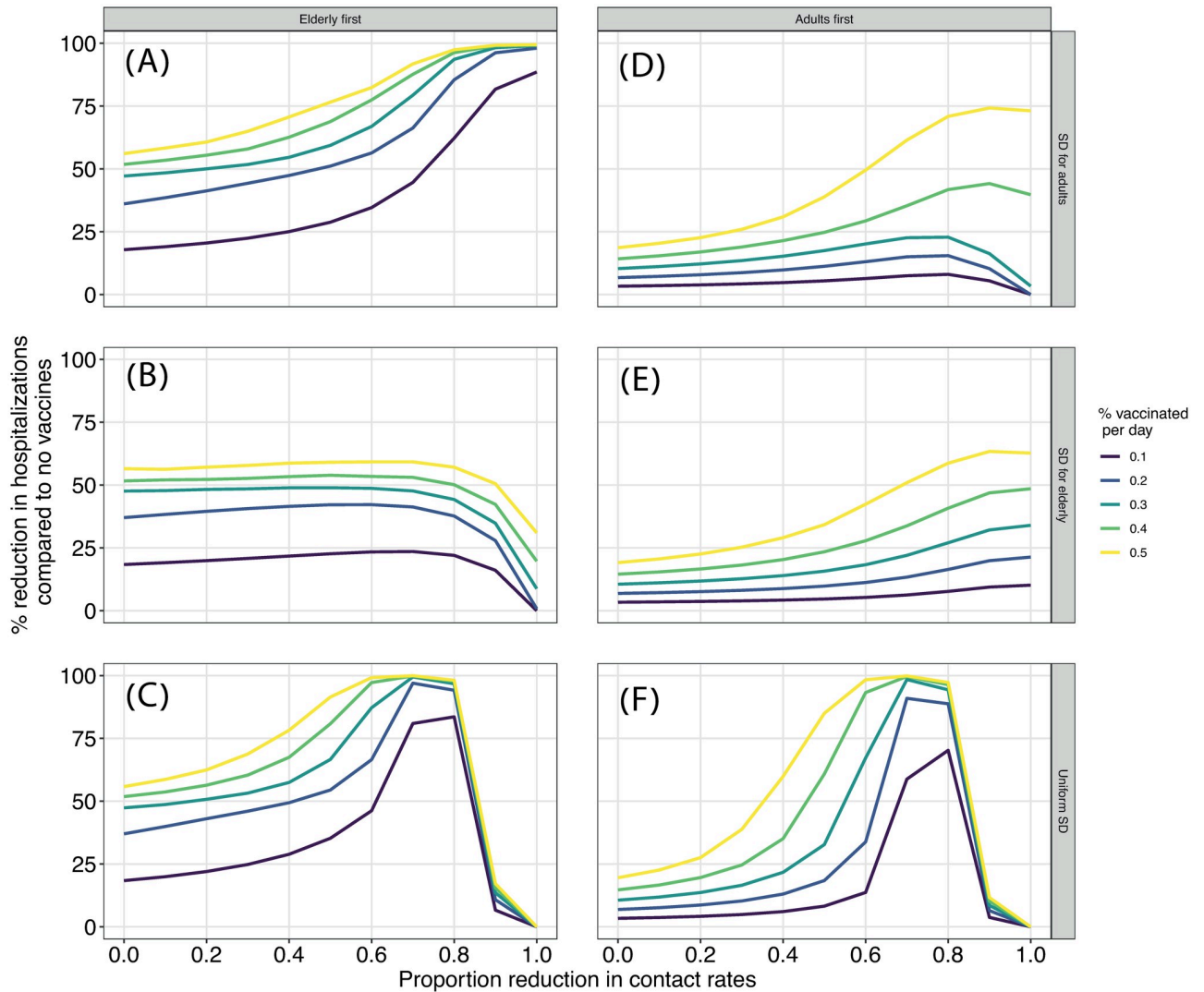
Fig 2. Effect of joint interventions on vaccination efficiency. The plot depicts F_H (y-axis) as a function of strength of social distancing (x-axis), vaccination rates (κ; line colors), vaccination strategies (columns) and social distancing strategies (rows).

Nevertheless, the elderly first strategy has overall lower P_H. In addition, under elderly first, a uniform or adult social distancing is preferred. A comparison to simulations in which the probability of hospitalizations (h_j) is uniform across all age groups indicates that age-dependent disease severity is a major factor underlying these patterns (S5 and S6 Figs).

To explore which vaccination strategy works better under different social distancing strategies in a systematic manner, we measured the difference in number of hospitalizations between the vaccination strategies as

$$D_H = \frac{H_a - H_e}{H_a},$$

(2)

where H_e and H_a are the total cumulative number of hospitalizations by the end of the simulation under the elderly first or adults first strategies, respectively (across ages) (S7 Fig). For
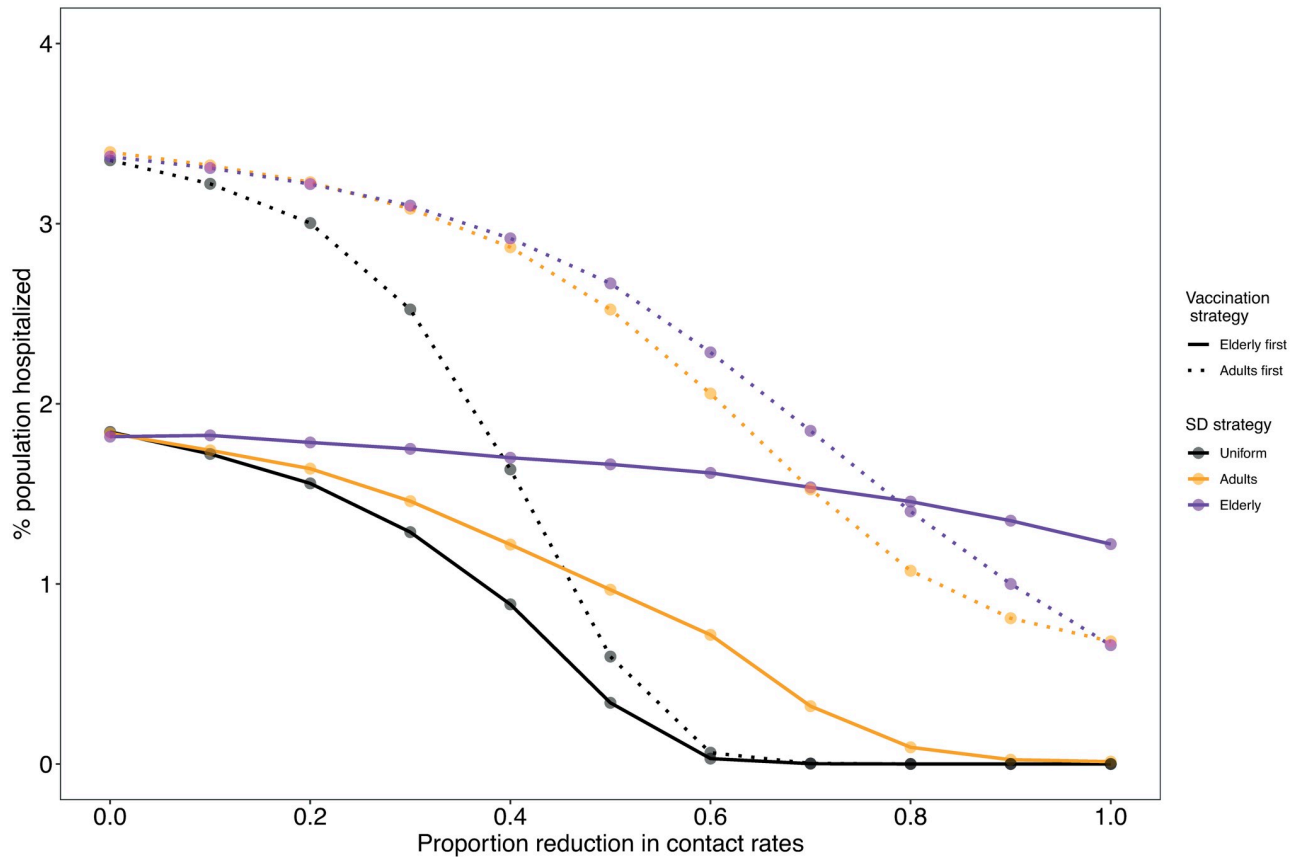
Fig 3. Effects of joint interventions on the proportion of the population hospitalized (P_H). Each data point represents a combination of a vaccination strategy (solid vs. dotted lines) and a social distancing strategy (colors) at particular social distancing strength (x-axis). Simulations were run using a daily deployment of $\kappa = 0.5\%$ of the population.

https://doi.org/10.1371/journal.pcbi.1009319.g003

example, if $H_e = 15,000$ and $H_a = 20,000$ then $D_H = 25\%$. Hence, $D_H > 0$ indicates that vaccinating elderly is preferred to adults.

We detect a general trend in which an elderly first strategy is preferable when combined with a uniform or adult-targeted social distancing (Fig 4). In tandem with our results on
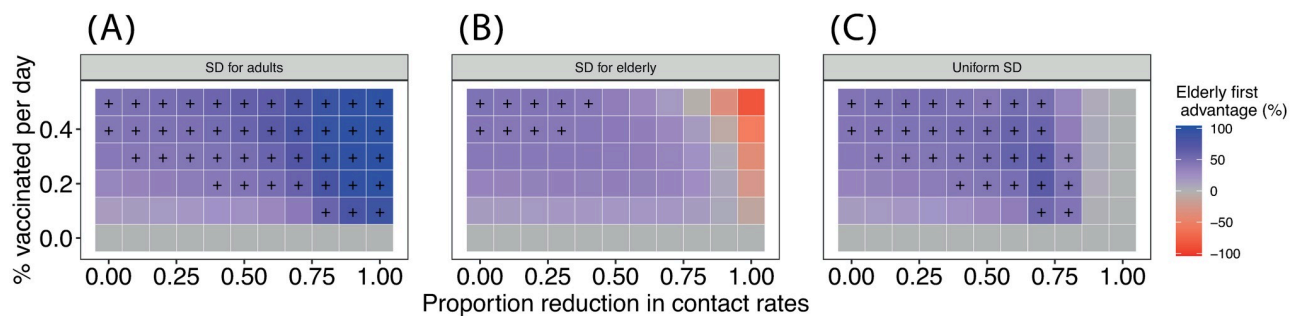
Fig 4. Systematic comparison between vaccination strategies in reducing hospitalizations. Each square in the heat maps depicts the percent difference in the number of hospitalizations between the two vaccination strategies ($D_H = (H_a - H_e)/H_a$; see text for explanation) for a given strength of social distancing (x-axis), vaccine deployment rate (κ, y-axis) and social distancing strategy (panels A-C). Color scale depicts the advantage of an elderly first strategy compared to an adults first strategy. Combinations higher than the median D_H are marked with a + sign. An example for the values underlying H_a and H_e for a 50% reduction in contacts can be found in S7 Fig.

https://doi.org/10.1371/journal.pcbi.1009319.g004

vaccine efficiency, under very strong social distancing ($\gtrsim 0.6$) targeted at the elderly, the effect of vaccination is overridden by that of social distancing, and vaccinating adults is preferred (Fig 4B). Finally, an elderly first strategy is mainly preferred in high vaccination rates when social distancing is low (Fig 4). This observation is crucial because it indicates that with low vaccination rates an elderly first strategy may have only a marginal benefit under some conditions. However, with moderate-high vaccination rates and social distancing targeted at adults, an elderly first strategy performs better than an adults first strategy, even under low levels of social distancing.

Reproductive number R_t depends on the combination of vaccination and social distancing

A key objective of interventions is to bring the number of active cases to a level that would prevent further transmission in the population. During the course of an epidemic, this is typically quantified using the reproductive number R_t, which is the time-varying analog of R_0. When R_t < 1 every person will infect on average less than one other person, indicating that the disease can no longer spread. We estimated R_t from simulation data using the method of [19] as recommended by [20]. This method is also used by the Israeli Ministry of Health. Briefly, R_t is calculated as

$$R_t = \frac{z_t}{\sum_{s=0}^{t} z_{t-s} w_s}.$$ (3)

In empirical data, z_t is the number of new infected individuals detected at day t but in our simulations we have full knowledge on active cases and use $z_t = I_t + A_t + P_t$. The denominator is the sum of the infection potential of those that were infected within the previous s days. It is calculated using w_s, which is a probability distribution for the interactivity profile, dependent on the time since infection. Following [21] and references therein, and the Israel Ministry of Health, we estimated w_s using a gamma distribution with a mean of 4.5 and standard deviation of 2.5, and calculated R_t over a period of $s = 7$ days.

Intuitively, the time it takes to reach $R_t = 1$ will be fastest when the disease is allowed to spread without any interventions because the amount of susceptible individuals decreases rapidly. We indeed observe this pattern (Fig 5A). Nevertheless, this is an undesired situation that will cost many lives. The goal is therefore not necessarily to bring R_t below 1 as fast as possible, but to reduce it to prevent massive infections and resulting hospitalizations. Social distancing significantly increases the time it takes to reach $R_t = 1$ (Fig 5) but lowers it. Vaccination positively interacts with social distancing, further reducing R_t, but only when vaccination rates are high enough. In our model, a daily deployment to 0.1% of the population has only a marginal benefit, whereas that of 0.5% significantly reduces R_t, especially when combined with a strong social distancing (Fig 5C). Interestingly, under uniform social distancing, which is the most common strategy applied, R_t is little affected by the vaccination strategy (see S8 Fig for other strategies).

Discussion

We used a deterministic compartmental model to mechanistically explore the qualitative interplay between vaccination and social-distancing on COVID19 disease dynamics. Strong social distancing keeps the number of susceptible individuals high but without a vaccine, infection and concomitant hospitalizations are inevitable. From a public health standpoint, social distancing and vaccination are short- and long-term interventions, respectively. Hence, a combination of these should provide greater benefits than when applied separately. We find that
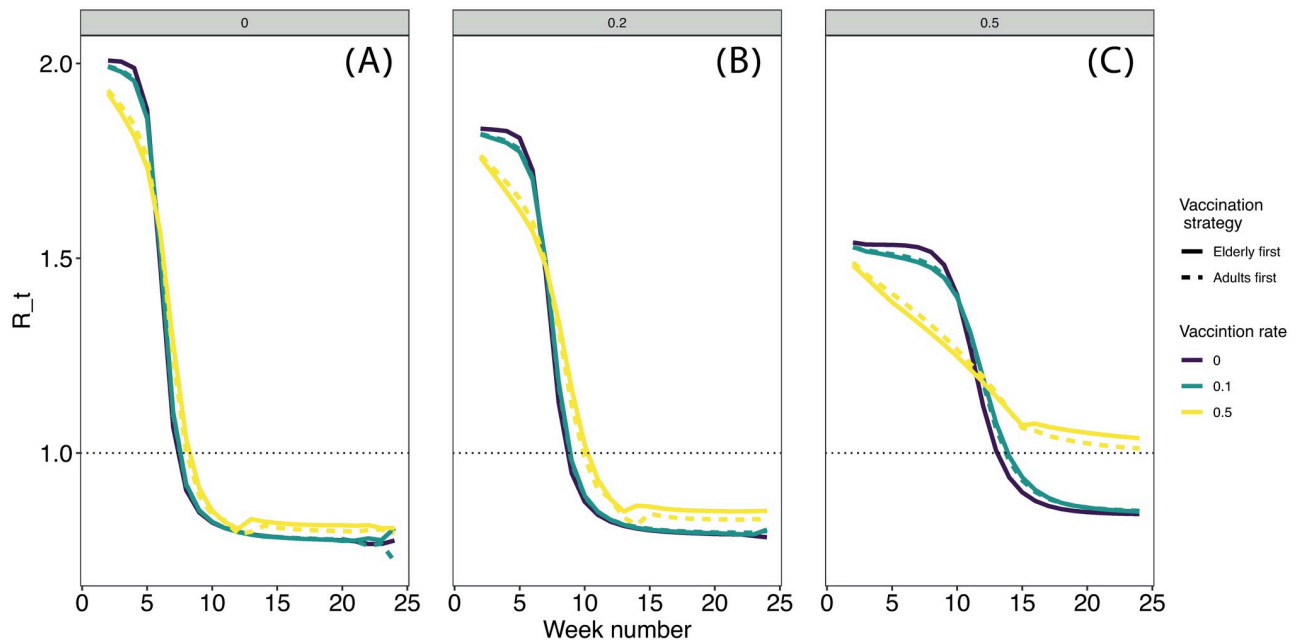
Fig 5. R_t for a uniform social distancing strategy. Each panel represents a proportion of reduction in contact rates: 0 (no social distancing, panel A), 0.2 (B), and 0.5 (C). R_t was calculated weekly (x-axis) as descried in the main text. Other social distancing strategies are presented in S8 Fig.

https://doi.org/10.1371/journal.pcbi.1009319.g005

synergism between interventions can indeed be obtained via particular combinations. For example, by prioritizing vaccines to elderly and applying social distancing to adults. However, there are also quantitative effects. Most notably, under low vaccination rates the elderly first strategy that has been found to be preferable (e.g., [11, 13]) may have only a marginal benefit over an adult first strategy, including for bringing R_t below 1, but increasing social distancing can increase this vaccination strategy's efficiency.

Modeling is instrumental to informing policy makers and the public about possible scenarios of disease progression and the potential efficacy of different intervention methods [17, 22–24]. Estimation of the parameters necessary for accurate modeling is improving considerably, including social parameters. For example, a recent study showed only about 70% vaccine acceptance in Israel [18]. In our simulations we found no qualitative difference in effect on hospitalizations between 70%, 80% and 100% acceptance (see sensitivity analyses) because deployment to individuals with vaccine hesitancy is obtained when infections may be close to their peak. An effect of vaccine hesitancy may be notable under higher rates of vaccination or within other modeling frameworks. Researchers should recognize limitations of this kind and that inaccurate parameterization or ignoring model assumptions (e.g., geographical heterogeneity) could potentially lead to erroneous conclusions [25]. Our model assumes homogeneous mixing in space and reflects an average population—for example, it does not include household, school, or work dynamics, which are relevant when investigating epidemic infections via contacts. Therefore, results should be considered qualitatively to provide general guidelines.

Nevertheless, when interpreted within the known limitations, our study provides valuable insights into the joint effect of vaccination and social distancing and the mechanisms underling their interplay. It also provides initial guidelines for policy makers. For example, for some

strategy combinations, vaccine efficiency varies little with increasing strength of social distancing, indicating that the social burden of social distancing may be relaxed. In addition, despite the synergism with social distancing, vaccination has little effect on R_t when deployed at low rates. This is because a vaccine is deployed during the pandemic, while non-vaccinated individuals continuously get infected. We considered deployment rates typical for the world average but the effect of vaccine should be more notable with higher deployment rates. In contrast to vaccination which reduces the number of susceptible individuals, social distancing increases the time to reach $R_t = 1$ because it only impedes infections. Therefore, social distancing is a strategy to "flatten the curve" but, as we show here, the way that it is applied and combined with vaccinations can change its outcomes.

As COVID19 vaccine is novel and its rollout urgent, clear guidelines on who to vaccinate have been constantly developing. For example, in Israel, at the beginning of deployment, vaccines were given to individuals who have not been confirmed as positive. Without population-wide serological surveys, this guideline is logical. The strict link between symptom history and vaccine eligibility in our study follows this guideline as we aim to model a scenario of limited vaccine availability with a need for prioritization. However, this may also be a model limitation, since in real life some fraction of those with asymptomatic infection may know their status via routine contact tracing or serological surveys. Moreover, guidelines may change as the public health community gains more experience and/or when availability increases. In Israel, the decision of vaccinating previously-positive individuals was given only after a major proportion of the eligible population has been vaccinated (pers. communication of co-author Davidovitch with COVID19 cabinet members.)

Our model contains, beyond an age structure and age-dependent contact matrices, all the main states of COVID19 and its implementation allows for flexible prioritization strategies: One can choose a certain order of age groups to vaccinate, and if the number of individuals to vaccinate at a certain group is depleted but there are still vaccines available, the model shifts dynamically to the next group. While these features have been used in separate studies, they have not been combined in a single framework of deterministic modeling. Our model is therefore an excellent tool to mechanistically test a range of hypotheses and strategies for interventions. For example, we did not include children in our targeted interventions because vaccine was not available for them at the time of writing, and to reduce the complexity of the study design. This is, however, a necessary future direction.

Vaccine prioritization is an ethical issue to which some guidelines have been laid out [8, 9]. We advocate for a mechanistic understanding of the factors that affect vaccination success and how to combine interventions in a way that will align with ethical guidelines. Our study provides insights towards these goals.

Methods

Ethics statement

All the data we use originates from publicly available resources, such as academic literature or online epidemiological sources. We do not use any clinical data that requires IRB.

Model structure

The model is a mass action model that reflects a situation in which the number of contacts is independent of the population size–a reasonable choice for directly-transmitted diseases [26]. It follows a population of N individuals, divided into nine age groups, depicted with the

subscript j (S1 Table) and is described in the following equations:

$$\frac{dS_j}{dt} = -\sum_l \beta_{jl}(I_l + A_l b + P_l b)\frac{S_j}{N_l} - \mu_j S_j \quad (4a)$$

$$\frac{dE_j}{dt} = \sum_l \beta_{jl}(I_l + A_l b + P_l b)\frac{S_j}{N_l} - \alpha E_j - \mu_j E_j \quad (4b)$$

$$\frac{dP_j}{dt} = \alpha E_j - \phi P_j - \mu_j P_j \quad (4c)$$

$$\frac{dI_j}{dt} = (1 - m_j)\phi P_j - \eta I_j \quad (4d)$$

$$\frac{dA_j}{dt} = m_j \phi P_j - \gamma A_j - \mu_j A_j \quad (4e)$$

$$\frac{dR_j}{dt} = (1 - h_j)\eta I_j \quad (4f)$$

$$\frac{dU_j}{dt} = \gamma A_j - \mu_j U_j \quad (4g)$$

$$\frac{dH_j}{dt} = h_j \eta I_j \quad (4h)$$

$$\frac{dV_j}{dt} = \mu_j(S_j + E_j + P_j + A_j + U_j) \quad (4i)$$

Model states and parameters

Parameters for this kind of model are of two kinds. First, "biological" parameters, the variation of which is less related to country-specific demographics. These include, for example, recovery time (γ), the probability of developing an asymptomatic disease (m), incubation period (α), time spent in a presymptomatic stage (ϕ) and age-dependent probability of hospitalization (h). We obtained these parameters from the literature (see below). Second, demographic "social" parameters that may vary between countries and include age structure and contact rates between age groups. We obtained age structure from https://unctadstat.unctad.org/wds. Below we detail model states and the parameters we use to transition between them (see S2 Table for a summary).

Infected states. Individuals start at a susceptible state (S) and become infected upon an encounter with infectious individuals that are either presymptomatic (P), symptomatic (I) or asymptomatic (A). Following [16], we include a "scaling parameter", b, ranging between 0–1 that determines the degree of infectiousness of states A and P compared to I (1 means a/presymptomatic are as infectious as symptomatic). We present results with $b = 0.5$ [16] but our results do not change qualitatively with other values. Infections occur at a rate specified by the infection matrix β_{lj}, which we calculated as the product of the infection probability q and contact rates between age groups j and l, given by the contact matrix C_{lj}. Therefore, $\beta_{lj} = q \cdot C_{lj}$ and we now detail how we obtained C_{lj} and q.

Infection parameters. We obtained C_{lj} for different countries from [27], which is currently the most comprehensive empirical (not inferred, e.g. [28]) survey of contacts relevant for the transmission of diseases such as COVID19, using the R package socialmixr. These contact matrices describe the daily mean number of contacts that participants have with people at different age groups (S9 Fig). We used the Italian contact network for Israel as a one for Israel

is not available but results were qualitatively consistent across countries, including Italy. Mossong et al. [27] defined physical contacts as those that included interactions such as a kiss or a handshake and nonphysical contacts as those involving being in close proximity for a certain amount of time (e.g., a two-way conversation without skin-to-skin contact). Because SARS-COV-2 can also be transmitted via air droplets and aerosols, we included all physical contacts and those non-physical contacts that lasted for 15 minutes or more. Infection due to an encounter with individuals from the same age group occurs when $l = j$. We halved the matrix diagonal to avoid counting the same interaction twice.

Estimating infection probability, q.   We calculated the average rate of infection $\hat{\beta}$ by fitting an exponential model of the form $I(t) = e^{(\hat{\beta}-\gamma)t}$ (sensu [29]) to Israeli case data across ages. This equation describes the invasion of the virus to a completely susceptible population at the early stages of the disease (days 1–35, before interventions were forced in Israel). This model gave a value of $\hat{\beta} = 0.38$ infections per day ($p < 0.001$, fit: $R^2 = 0.98$). Estimating $\hat{\beta}$ from R_0 gave a similar estimate of 0.41 and this difference does not affect the results (see sensitivity analysis). Because $\hat{\beta}$ is an average across all the population, we calculated the infection probability given an encounter between a susceptible and infected individuals as $q = \hat{\beta}/ < C_{lj} >$. We then incorporated the recent estimates by [21] that children ages 0–20 are 43% less susceptible and 63% less infected than adults by reducing q for these ages proportionally.

Parameters of infection progression.   Upon infection, the virus has an average latency period of 6.4 days ($\alpha = 1/6.4$) [30]. Individuals remain in presymptomatic stage for an average of 2.1 days ($\phi = 1/2.1$) [31], after which individuals become either asymptomatic with a probability m_j or develop symptoms with probability $1 - m_j$. The fraction of asymptomatic COVID19 infections was estimated at 30–40% [32]. In the absence of data on age-specific asymptomatic infections [16], we have set $m = m_j = 0.4$ for all ages. However, our model retains the flexibility to quantify the role of age-dependent asymptomatic probabilities in COVID19 epidemiology (m_j) because a previous study on corona viruses (not including SARS-COV-2) found that children tend to be less symptomatic than adults [33].

Parameters for infection outcomes.   Asymptomatic individuals stop infecting (U) within 7 days ($\gamma = 1/7$)—an estimate from [34] that lies between that of [31] (mean 5 days) and that of [35] (mean 11 days). Results were qualitatively the same when we used the estimate by Davies et al [31], also used in [11]. We assume that symptomatic individuals are identified and removed to quarantine (R) within 1 day ($\eta = 1$). Depending on age, with probability h_j individuals can develop severe symptoms and be hospitalized (H). Therefore, H_j represents the cumulative number of hospitalized individuals at any given time. We calculated h_j using data from [36] as the fraction of hospitalized cases out of all cases (see S1 Table for details). This probability is not expected to vary greatly between countries as age-dependent hospitalization has a strong biological rather than social component in countries which are culturally similar. Effectively, individuals in states V, U, R and H cannot further infect. Separating between R and U is useful for scenarios in which quarantine should be considered separately from asymptomatic recovery (e.g., for economic reasons because some quarantined individuals cannot work).

Interventions

Vaccination.   We administer vaccines to people in states S, E, P, A and U, as they do not show symptoms and are therefore considered susceptible from a public health perspective. We assume the vaccine prevents infection as well as disease, has an efficiency of 95%, and affects all individuals in the same way. Vaccines are deployed from the beginning of the

simulation at a constant rate of κ vaccines per day, which we set as the percentage of the total population that a government can vaccinate a day. For example, in Israel (population about 8.7 million), vaccinating 0.2% of the population every day translates into deployment of about 17400 vaccines daily and over 1.5 million vaccines in the course of 90 days. We use values of κ ranging from 0.1% to 0.5%. The current rate at the EU, for example is 0.2–0.3%, and the world average is 0.1% (https://ourworldindata.org/covid-vaccinations).

In our simulations κ is first divided across the target age groups in proportion to the number of people left to vaccinate in each group (κ_j). Then, the rate of vaccination (vaccines per person per day) is calculated as:

$$\mu_j(t) = \frac{\kappa_j}{S_j + E_j + P_j + A_j + U_j} e \quad (5)$$

where e is vaccine efficiency, set to 95% [37].

Social distancing. Social distancing is the act of reducing contacts. Hence, we define $\beta_{lj}^S = (1 - x_{lj})\beta_{lj}$, where elements of x_{lj} range between 0 (no social distancing) and 1 (no contacts whatsoever), and act to reduce contacts within and between groups. x_{lj} is the quantity depicted on the x-axis of figures (e.g., Fig 2). We note that the multiplication $x_{lj}\beta_{lj}$ is an element-by-element multiplication rather than a matrix multiplication and that intervention is symmetric. For example, $x_{1,1} = 0.4$ will reduce contacts between juveniles within the age group 0–9 to 60% of the non-intervention level and $x_{3,1} = x_{1,3} = 0.9$ is a strong social distancing intervention reducing contacts between age groups 0–9 and 20–29 to 10% of their non-intervention level.

Model implementation and sensitivity analyses

We implement the mathematical model with the package deSolve in R [38]. To facilitate future studies and study replication, we have developed a pipeline that allows changing parameters and running the model on High Performance Computing systems or locally with relative ease. This is described in the GitHub repository.

We run simulations for 24 weeks and have conducted multiple sensitivity analyses for the following parameters: γ, α, ϕ, η, b, and the proportion vaccinated (70% and 100% acceptance). For β, we tried an alternative estimation by calculating the R_0 for Israel (across ages) using the method of [39] implemented in the R package R0 [40]. We used case data on days 1–35, before interventions were forced because R_0 describes the invasion of the virus to a completely susceptible population at the early stages of the disease. This analysis gave an $R_0 = 2.9$. We then calculated $\hat{\beta} = R_0/\gamma = 0.41$ [26]. Qualitatively, our results for all sensitivity analyses were robust to changes in these parameters. We also repeated our analyses for Belgium, Germany and Italy using R_0 estimates from [41], and obtained similar results. Finally, calculating R_t using the method of [39] did not change the results qualitatively. Outputs of all these simulations can be found in the GitHub repository, along with the code.

Supporting information

S1 Fig. Epidemiological curves without vaccine. Epidemiological curves for the baseline model, with no vaccination or social distancing. The model follows a population divided to nine age groups as depicted in the figure. S: susceptible; E: exposed; P: presymptomatic; I: infectious and symptomatic; A: infectious and asymptomatic; R: removed to quarantine and then recovered naturally, and immune; U: recovered naturally, and immune; H: hospitalized. (PDF)

S2 Fig. Epidemiological curves with vaccine. Epidemiological curves with vaccination ($\kappa = 0.2$) and no social distancing. The model follows a population divided to nine age groups as depicted in the figure. S: susceptible; E: exposed; P: presymptomatic; I: infectious and symptomatic; A: infectious and asymptomatic; R: removed to quarantine and then recovered naturally, and immune; U: recovered naturally, and immune; H: hospitalized; V: vaccinated.
(PDF)

S3 Fig. Comparison of dynamics between two prioritization strategies. Dashed and solid lines depict two strategies, respectively: (i) vaccinating all elderly (60+) and then all adults (20-59) and (ii) vaccinating all adults and then all elderly. This example is for $\kappa = 0.5$ (0.5% of the population is vaccinated per day), with no social distancing. In the first strategy, after about 35 days there are no more elderly to vaccinate and the model shifts to vaccinating adults (gray dashed line). In the second strategy, the switch to vaccinating elderly occurs after about 75 days because the number of adults in the population is larger than that of elderly. Most of the reduction in hospitalizations is obtained when the elderly are prioritized (compare black lines). I: infectious and symptomatic (red); H: hospitalized (black); V: vaccinated (gray).
(PDF)

S4 Fig. Comparison of control to vaccine intervention. Dashed lines depict control (no vaccine). Solid lines depict a strategy in which we first vaccinate elderly (60+) and then adults (20-59). In this example we use $\kappa = 0.4$ (0.4% of the population is vaccinated per day) and there is no social distancing. After about 25 days there are no more elderly to vaccinate and the model shifts to vaccinating adults (gray solid line). It is clear that most of the reduction in hospitalizations is obtained for the elderly groups (compare dashed to solid black lines). The orange and green dots mark the $H_{j(\kappa=0.4)}$ and H_j^0 values (for $j = 80+$) used in [Eq 1](Eq 1) in the main text, respectively. Model was run for 30 weeks but 12 weeks are plotted here for clarity. I: infectious and symptomatic (red); H: hospitalized (black); V: vaccinated (gray).
(PDF)

S5 Fig. Effect of joint interventions on the proportion of hospitalization using age-uniform hospitalization probabilities. The plot depicts P_H (y-axis) as a function of strength of social distancing (x-axis), vaccination rates (κ; line colors), vaccination strategies (columns) and social distancing strategies (rows).
(PDF)

S6 Fig. Effects of joint interventions on the proportion of the population hospitalized (P_H) using age-uniform hospitalization probabilities. Each data point represents a combination of vaccination strategy (solid vs. dotted lines), social distancing strategy (colors) at particular social distancing strength (x-axis). Simulations were run for daily deployment of $\kappa = 0.5$% of the population. The probability of hospitalization was equal to the mean probability across ages (i.e., mean of h_j).
(PDF)

S7 Fig. Accumulation curves of hospitalizations. Columns and rows represent social distancing and vaccination strategies, respectively. This example is for a 50% reduction in contacts. The dashed lines mark the total number of hospitalizations for a $\kappa = 0.5$ vaccination rate. For example, under the adult social distancing scenario, $H_a = 219,882$ and $H_e = 84,321$.
(PDF)

S8 Fig. R_t for different social distancing strategies. Columns represent three levels of proportion of reduction in contact rates: 0 (no reduction), 0.2, and 0.5. Each row is a social distancing

strategy. R_t was calculated for 7-day periods as descried in the main text.
(PDF)

S9 Fig. An example of age-dependent contact rates. (A) Contact matrix for Italy calculated from data collected by Mossong et al. (2008). Matrix cells depict the mean number of daily contacts between people in different age groups. Diagonal cells depict contacts between individuals from the same age group. (B) The same data as in (A), represented as a network of contacts. Edge widths depict contact rates.
(PDF)

S1 Table. Population structure of Israel and relevant parameters.
(PDF)

S2 Table. Study parameters.
(PDF)

Acknowledgments

Author Contributions

Conceptualization: Sharon Guerstein, Rami Puzis, Shai Pilosof.

Data curation: Oren Miron.

Formal analysis: Sharon Guerstein, Victoria Romeo-Aznar, Shai Pilosof.

Funding acquisition: Nadav Davidovitch, Rami Puzis, Shai Pilosof.

Investigation: Sharon Guerstein, Victoria Romeo-Aznar, Oren Miron, Nadav Davidovitch, Rami Puzis, Shai Pilosof.

Methodology: Sharon Guerstein, Victoria Romeo-Aznar, Ma'ayan Dekel, Shai Pilosof.

Project administration: Shai Pilosof.

Resources: Shai Pilosof.

Software: Ma'ayan Dekel, Shai Pilosof.

Supervision: Shai Pilosof.

Visualization: Ma'ayan Dekel, Shai Pilosof.

Writing – original draft: Sharon Guerstein, Rami Puzis, Shai Pilosof.

Writing – review & editing: Sharon Guerstein, Victoria Romeo-Aznar, Nadav Davidovitch, Rami Puzis, Shai Pilosof.

References

1. Lee BY, Brown ST, Korch GW, Cooley PC, Zimmerman RK, Wheaton WD, et al. A computer simulation of vaccine prioritization, allocation, and rationing during the 2009 H1N1 influenza pandemic. Vaccine. 2010; 28(31):4875–4879. https://doi.org/10.1016/j.vaccine.2010.05.002 PMID: 20483192

2. Barrot JN, Grassi B, Sauvagnat J. Sectoral Effects of Social Distancing; 2020.

3. Venkatesh A, Edirappuli S. Social distancing in covid-19: what are the mental health implications? BMJ. 2020; 369:m1379. PMID: 32253182

4. Balicer RD, Huerta M, Davidovitch N, Grotto I. Cost-benefit of stockpiling drugs for influenza pandemic. Emerg Infect Dis. 2005; 11(8):1280–1282. https://doi.org/10.3201/eid1108.041156 PMID: 16102319

5. Khamsi R. If a coronavirus vaccine arrives, can the world make enough. Nature. 2020; 580(7805):578. https://doi.org/10.1038/d41586-020-01063-8 PMID: 32273621

6. Matrajt L, Eaton J, Leung T, Brown ER. Vaccine optimization for COVID-19, who to vaccinate first? Science Adv. 2020. https://doi.org/10.1126/sciadv.abf1374

7. Gallagher ME, Sieben AJ, Nelson KN, Kraay ANM, Lopman B, Handel A, et al. Considering indirect benefits is critical when evaluating SARS-CoV-2 vaccine candidates. medRxiv. 2020. https://doi.org/10.1101/2020.08.07.20170456 PMID: 32817958

8. Cohen J. The line is forming for a COVID-19 vaccine. Who should be at the front. Science. 2020; 369 (6499):15–16.

9. Emanuel EJ, Persad G, Kern A, Buchanan A, Fabre C, Halliday D, et al. An ethical framework for global vaccine allocation. Science. 2020; 369(6509):1309–1312. https://doi.org/10.1126/science.abe2803 PMID: 32883884

10. Foy BH, Wahl B, Mehta K, Shet A, Menon GI, Britto C. Comparing COVID-19 vaccine allocation strategies in India: A mathematical modelling study. Int J Infect Dis. 2021; 103:431–438. https://doi.org/10.1016/j.ijid.2020.12.075 PMID: 33388436

11. Bubar KM, Reinholt K, Kissler SM, Lipsitch M, Cobey S, Grad YH, et al. Model-informed COVID-19 vaccine prioritization strategies by age and serostatus. Science. 2020.

12. Buckner JH, Chowell G, Springborn MR. Optimal Dynamic Prioritization of Scarce COVID-19 Vaccines. medRxiv. 2020.

13. Jentsch P, Anand M, Bauch CT. Prioritising COVID-19 vaccination in changing social and epidemiological landscapes; 2020.

14. Yang J, Zheng W, Shi H, Yan X, Dong K, You Q, et al. Who should be prioritized for COVID-19 vaccination in China? A descriptive study. BMC Med. 2021; 19(1):45. https://doi.org/10.1186/s12916-021-01923-8 PMID: 33563270

15. Moghadas SM, Fitzpatrick MC, Sah P, Pandey A, Shoukat A, Singer BH, et al. The implications of silent transmission for the control of COVID-19 outbreaks. Proc Natl Acad Sci U S A. 2020; 117(30):17513–17515. https://doi.org/10.1073/pnas.2008373117 PMID: 32632012

16. Subramanian R, He Q, Pascual M. Quantifying asymptomatic infection and transmission of COVID-19 in New York City using observed cases, serology, and testing capacity. Proc Natl Acad Sci U S A. 2021; 118(9). https://doi.org/10.1073/pnas.2019716118 PMID: 33571106

17. Ferguson N, Laydon D, Nedjati Gilani G, Imai N, Ainslie K, Baguelin M, et al. Impact of non-pharmaceutical interventions (NPIs) to reduce COVID-19 mortality and healthcare demand. Imperial College; 2020.

18. Dror AA, Eisenbach N, Taiber S, Morozov NG, Mizrachi M, Zigron A, et al. Vaccine hesitancy: the next challenge in the fight against COVID-19. Eur J Epidemiol. 2020; 35(8):775–779. https://doi.org/10.1007/s10654-020-00671-y PMID: 32785815

19. Cori A, Ferguson NM, Fraser C, Cauchemez S. A new framework and software to estimate time-varying reproduction numbers during epidemics. Am J Epidemiol. 2013; 178(9):1505–1512. https://doi.org/10.1093/aje/kwt133 PMID: 24043437

20. Gostic KM, McGough L, Baskerville EB, Abbott S, Joshi K, Tedijanto C, et al. Practical considerations for measuring the effective reproductive number, Rt. PLoS Comput Biol. 2020; 16: e1008409. https://doi.org/10.1371/journal.pcbi.1008409 PMID: 33301457

21. Dattner I, Goldberg Y, Katriel G, Yaari R, Gal N, Miron Y, et al. The role of children in the spread of COVID-19: Using household data from Bnei Brak, Israel, to estimate the relative susceptibility and infectivity of children. PLoS Comput Biol. 2021; 17(2):e1008559. https://doi.org/10.1371/journal.pcbi.1008559 PMID: 33571188

22. Colbourn T. COVID-19: extending or relaxing distancing control measures. Lancet Public Health. 2020; 5(5):e236–e237. https://doi.org/10.1016/S2468-2667(20)30072-4 PMID: 32220654

23. Karin O, Bar-On YM, Milo T, Katzir I, Mayo A, Korem Y, et al. Adaptive cyclic exit strategies from lockdown to suppress COVID-19 and allow economic activity. medRxiv. 2020; (medrxiv;2020.04.04.20053579v4).

24. Prem K, Liu Y, Russell TW, Kucharski AJ, Eggo RM, Davies N, et al. The effect of control strategies to reduce social mixing on outcomes of the COVID-19 epidemic in Wuhan, China: a modelling study. Lancet Public Health. 2020; 5(5):e261–e270. https://doi.org/10.1016/S2468-2667(20)30073-6 PMID: 32220655

25. Holmdahl I, Buckee C. Wrong but Useful—What Covid-19 Epidemiologic Models Can and Cannot Tell Us; 2020.

26. Keeling MJ, Rohani P. Modeling infectious diseases in humans and animals. Keeling MJ, Rohani P, editors. Princetone, New Jersey: Princeton University Press; 2008.

27. Mossong J, Hens N, Jit M, Beutels P, Auranen K, Mikolajczyk R, et al. Social contacts and mixing patterns relevant to the spread of infectious diseases. PLoS Med. 2008; 5(3):e74. https://doi.org/10.1371/journal.pmed.0050074 PMID: 18366252

28. Prem K, Cook AR, Jit M. Projecting social contact matrices in 152 countries using contact surveys and demographic data. PLoS Comput Biol. 2017; 13(9):e1005697. https://doi.org/10.1371/journal.pcbi.1005697 PMID: 28898249

29. Dehning J, Zierenberg J, Spitzner FP, Wibral M, Neto JP, Wilczek M, et al. Inferring change points in the spread of COVID-19 reveals the effectiveness of interventions. Science. 2020; 369(6500). https://doi.org/10.1126/science.abb9789 PMID: 32414780

30. Backer JA, Klinkenberg D, Wallinga J. Incubation period of 2019 novel coronavirus (2019-nCoV) infections among travellers from Wuhan, China, 20-28 January 2020. Euro Surveill. 2020; 25(5). https://doi.org/10.2807/1560-7917.ES.2020.25.5.2000062 PMID: 32046819

31. Davies NG, Klepac P, Liu Y, Prem K, Jit M, CMMID COVID-19 working group, et al. Age-dependent effects in the transmission and control of COVID-19 epidemics. Nat Med. 2020; 26(8):1205–1211. https://doi.org/10.1038/s41591-020-0962-9 PMID: 32546824

32. Lavezzo E, Franchin E, Ciavarella C, Cuomo-Dannenburg G, Barzon L, Del Vecchio C, et al. Suppression of a SARS-CoV-2 outbreak in the Italian municipality of Vo'. Nature. 2020; 584(7821):425–429. https://doi.org/10.1038/s41586-020-2488-1 PMID: 32604404

33. Galanti M, Birger R, Ud-Dean M, Filip I, Morita H, Comito D, et al. Rates of asymptomatic respiratory virus infection across age groups. Epidemiol Infect. 2019; 147:e176. https://doi.org/10.1017/S0950268819000505 PMID: 31063096

34. Cheng HY, Jian SW, Liu DP, Ng TC, Huang WT, Lin HH, et al. Contact Tracing Assessment of COVID-19 Transmission Dynamics in Taiwan and Risk at Different Exposure Periods Before and After Symptom Onset. JAMA Intern Med. 2020; 180(9):1156–1163. https://doi.org/10.1001/jamainternmed.2020.2020 PMID: 32356867

35. Zou L, Ruan F, Huang M, Liang L, Huang H, Hong Z, et al. SARS-CoV-2 Viral Load in Upper Respiratory Specimens of Infected Patients. N Engl J Med. 2020; 382(12):1177–1179. https://doi.org/10.1056/NEJMc2001737 PMID: 32074444

36. Florida Department of Health. Florida Department of Health Open Data;. https://open-fdoh.hub.arcgis.com/datasets/florida-covid19-case-line-data-3/data.

37. Polack FP, Thomas SJ, Kitchin N, Absalon J, Gurtman A, Lockhart S, et al. Safety and Efficacy of the BNT162b2 mRNA Covid-19 Vaccine. N Engl J Med. 2020; 383(27):2603–2615. https://doi.org/10.1056/NEJMoa2034577 PMID: 33301246

38. Soetaert K, Petzoldt T, Setzer RW. Solving Differential Equations in R: Package deSolve; 2010.

39. Wallinga J, Lipsitch M. How generation intervals shape the relationship between growth rates and reproductive numbers. Proc Biol Sci. 2007; 274(1609):599–604. https://doi.org/10.1098/rspb.2006.3754 PMID: 17476782

40. Boelle PY, Obadia T. R0: Estimation of R0 and Real-Time Reproduction Number from Epidemics; 2015.

41. Ke R, Romero-Severson E, Sanche S, Hengartner N. Estimating the reproductive number R0 of SARS-CoV-2 in the United States and eight European countries and implications for vaccination. J Theor Biol. 2021; 517:110621. https://doi.org/10.1016/j.jtbi.2021.110621 PMID: 33587929